Physics Letters B 829 (2022) 137129

Contents lists available at ScienceDirect

Physics Letters B

www.elsevier.com/locate/physletb

First observation of a shape isomer and a low-lying strongly-coupled prolate band in neutron-deficient semi-magic ^{187}Pb

W.Q. Zhang [a,b], A.N. Andreyev [c,d,*], Z. Liu [a,b,**], D. Seweryniak [e], H. Huang [a,b], Z.H. Li [f], J.G. Li [a,f], C.Y. Guo [f], D.T. Doherty [g], A.E. Barzakh [h], P. Van Duppen [i], J.G. Cubiss [c], B. Andel [j], S. Antalic [j], M. Block [k,l,m], A. Bronis [j], M.P. Carpenter [e], P. Copp [e], B. Ding [a,b], Z. Favier [n], F. Giacoppo [k,l], T.H. Huang [a,b,e], X.H. Yu [a,b], B. Kindler [l], F.G. Kondev [e], T. Lauritsen [e], G.S. Li [a,b], B. Lommel [l], H.Y. Lu [a,b], M. Al Monthery [c], P. Mošať [j], Y.F. Niu [o], C. Raison [c], W. Reviol [e], G. Savard [e], S. Stolze [e], G.L. Wilson [p], H.Y. Wu [f], Z.H. Wang [o], F.R. Xu [f], Q.B. Zeng [a,b], X.H. Zhou [a,b]

[a] Institute of Modern Physics, Chinese Academy of Sciences, Lanzhou 730000, China
[b] University of Chinese Academy of Sciences, Beijing 100049, China
[c] Department of Physics, University of York, York, YO10 5DD, United Kingdom
[d] Advanced Science Research Center (ASRC), Japan Atomic Energy Agency, Tokai-mura, Japan
[e] Physics Division, Argonne National Laboratory, Argonne, IL 60439, USA
[f] State Key Laboratory of Nuclear Physics and Technology, School of Physics, Peking University, Beijing 100871, China
[g] Department of Physics, University of Surrey, Guildford, GU2 7XH, United Kingdom
[h] Petersburg Nuclear Physics Institute, NRC Kurchatov Institute, 188300 Gatchina, Russia
[i] KU Leuven, Instituut voor Kern- en Stralingsfysica, 3001 Leuven, Belgium
[j] Department of Nuclear Physics and Biophysics, Comenius University in Bratislava, 84248 Bratislava, Slovakia
[k] Helmholtz-Institut Mainz, Mainz, 55128, Germany
[l] GSI Helmholtzzentrum für Schwerionenforschung Darmstadt, Darmstadt, 64291, Germany
[m] Johannes-Gutenberg Universität, Mainz, 55099, Germany
[n] Physics Department, CERN, 1211 Geneva 23, Switzerland
[o] Lanzhou University, Lanzhou 730000, China
[p] Department of Physics and Astronomy, Louisiana State University, Baton Rouge, LA 70803, USA

ARTICLE INFO

Article history:
Received 2 November 2021
Received in revised form 22 March 2022
Accepted 22 April 2022
Available online 27 April 2022
Editor: B. Blank

Keywords:
Isomeric state
Rotational band
Shape coexistence
PES calculations

ABSTRACT

Prompt and delayed γ-ray spectroscopy of the neutron-deficient, semi-magic isotope ^{187}Pb has been performed using the recoil-decay and isomer-decay tagging techniques at the Argonne Gas-Filled Analyzer. A new 5.15(15)-μs isomeric state at only 308 keV above the spherical $3/2^-$ ground state is identified and classified as a shape isomer. A strongly-coupled band is observed on top of the isomer, which is nearly identical to the one built on the prolate $7/2^-[514]$ Nilsson state in the isotone ^{185}Hg. Based on this similarity and on the result of the potential-energy surface calculations, the new isomer in ^{187}Pb is proposed to originate from the same configuration. The retarded character of the 308-keV $(7/2^-) \rightarrow 3/2^-_{gs}$ transition with a deduced $B(E2) = 5.6(2) \times 10^{-4}$ W.u. can be well explained by the significant difference between the prolate parent and spherical daughter configurations, leading to the shape isomerism. The excitation energy of the isomer is surprisingly low, being roughly half of the excitation energies of the known 0^+ intruder bandheads in the neighboring ^{186,188}Pb isotopes. The combined results of the present work and the previous α-decay and laser spectroscopy studies present evidence for triple shape coexistence at low energy in the negative-parity configurations of ^{187}Pb, which is well reproduced by the potential-energy surface calculations.

1. Introduction

The coexistence of different shapes at low excitation energies within the same nucleus is a well-established phenomenon in the vicinity of closed shells, exhibiting the complexity of the nu-

* Corresponding author at: Department of Physics, University of York, York, YO10 5DD, United Kingdom.
** Corresponding author at: Institute of Modern Physics, Chinese Academy of Sciences, Lanzhou, 730000, China.
E-mail addresses: andrei.andreyev@york.ac.uk (A.N. Andreyev),

https://doi.org/10.1016/j.physletb.2022.137129

cleus as a quantum many-fermion system [1,2]. It is well known that nonspherical shapes in nuclei are induced by the residual interactions between valence protons and neutrons. Shape coexistence can occur when one or more valence nucleons of one type occupy deformation driving ("intruder" - in the language of the shell model) orbitals and consequently "polarize" the nucleus towards deformation through interacting with valence nucleons of the other type.

Some of the best examples of shape coexistence were observed in the neutron-deficient semi-magic Pb ($Z = 82$) isotopes in the vicinity of the $N = 104$ neutron midshell, in which the spherical, oblate and prolate configurations co-exist at excitation energies [3–5]. For example, a triplet of low-lying shape-coexisting 0^+ states was found in ^{186}Pb, in which the two deformed excited states are only ∼600 keV above the spherical ground state (gs) [4]. Strong complementary evidence for shape coexistence can also be obtained from studies of high-spin isomers, as was shown in ^{188}Pb via the identification of several differently-shaped isomeric states [6]. In parallel with extensive experimental work, numerous theoretical investigations have been performed employing the complementary spherical shell model and deformed mean-field approaches [7–9]. Furthermore, the beyond mean-field and relativistic mean-field theories are also frequently used in neutron-deficient Pb isotopes [10].

In contrast to the well studied even-even Pb isotopes, little information is available regarding shape coexistence in the odd-A Pb nuclides. Two α/β-decaying states are known in the $^{183-199}$Pb isotopes around the neutron mid-shell: the $3/2^-_{gs}$ associated with the $\nu p_{3/2}$ configuration and the excited $13/2^+$ isomer from the $\nu i_{13/2}$ orbital. The bands built on the $13/2^+$ isomers were observed due to the dominant population of high-spin states in complete-fusion reactions, e.g. in-beam studies of ^{185,187,189}Pb [11–14]. However, only sparse data are available for low-spin excited states, identified via α decay of parent odd-A isotopes, $^{187-195}$Po [15–18].

The present study focuses on ^{187}Pb ($N = 105$), for which there is relatively little information currently available. The α-decay half-life, energy, and branching ratio evaluated previously for the $3/2^-_{gs}$ of ^{187}Pb are 15.2(3) s, 6194(10) / 5993(10) keV, and 9.5(20)%, respectively, and for the $13/2^+$ isomer are 18.3(3) s, 6077(7) keV and 12(2)%, respectively [19–21]. Both the gs and the isomer were found to be nearly spherical by laser spectroscopy studies at ISOLDE [22]. A sequence of three γ-ray transitions of 831, 416 and 476 keV was observed in the in-beam studies on top of the $13/2^+$ state [12]. Several excited states in ^{187}Pb were identified in α-decay investigations of ^{191m,g}Po [23,17]. Based on the α decay hindrance factors and on systematics in neighboring nuclei, it was proposed that one of them, with $I^\pi = (3/2^-)$ at 375.0(10) keV relative to the $3/2^-_{gs}$, has an oblate configuration. Meanwhile, the $(13/2^+)$ state at 494.0(10) keV relative to the $13/2^+$ isomer, was proposed as a bandhead of an oblate intruder band and a state with $I^\pi = (9/2^+)$ at 472.0(10) keV relative to the $13/2^+$ isomer, as a bandhead of a prolate $9/2^+[624]$ band [23,17]. So far no rotational band structures have be observed experimentally in ^{187}Pb.

In this Letter, we report on the observation of a new 5.15(15)-μs isomeric state with $I^\pi = (7/2^-)$ at 307.9(1) keV above the $3/2^-_{gs}$ of ^{187}Pb, and of a prolate rotational band built on top of this isomer. These data establish a pronounced shape coexistence phenomenon in ^{187}Pb, which is also supported by the potential-energy surface (PES) calculations. The rotational band is proposed to arise from the strong coupling of the neutron occupying $7/2^-[514]$ Nilsson orbital to the deformed core corresponding to a prolate PES minimum in ^{186}Pb. This is the first observation of a surprisingly low-lying negative-parity, strongly-deformed band in the light odd-A semi-magic Pb isotopes, for which the bandhead energy is about half of the excitation energies of the corresponding 0^+ intruder bandheads in ^{186,188}Pb.

2. Experiment and results

The ^{187}Pb nuclei were produced in the ^{50}Cr + ^{142}Nd → ^{192}Po* → ^{187}Pb + 2p3n reaction. A 255-MeV ^{50}Cr beam with a typical intensity of 7 pnA was delivered by the ATLAS superconducting linear accelerator. The target was made from isotopically enriched $^{142}NdF_3$ material (99.8% enrichment and 700-μg/cm^2 thickness including F element). Four target sectors were mounted on a rotating wheel, and the beam was wobbled around ±2.5 mm horizontally across the target by a magnetic steerer to reduce the heating of the target.

Evaporation residues (EVRs) were separated from the primary beam by the Argonne Gas-Filled Analyzer (AGFA) [24] filled with 0.65 mbar of helium gas. A position sensitive parallel grid avalanche counter (PGAC), located at the exit of the separator, provided time of arrival and energy-loss signals of EVRs. They were subsequently implanted into a 300-μm thick, 64 mm × 64 mm (160 × 160 strips) double-sided silicon strip detector (DSSD) located 40 cm behind the PGAC. The DSSD was used to detect the implantation of EVRs and their subsequent particle decays, and allowed for the standard temporal and spatial recoil-decay correlation techniques to be applied. The DSSD was calibrated by using the α decay of implanted ^{186,187}Pb, $^{183-185}$Hg, and ^{188,189}Bi [25]. The typical energy resolution for the DSSD was about 30 keV (FWHM) in the energy range of 5000–7000 keV. Four clover HPGe detectors (X-array) [26] consisting of 4 crystals each were installed surrounding the DSSD chamber for prompt and delayed EVRs-γ and α-γ coincidence measurements. The typical energy resolution for the X-array was ∼3.6 keV (FWHM) for γ-ray energies around 300 keV.

Prompt γ rays at the target position were detected by the Gammasphere (GS) array [27] with 64 large-volume Compton-suppressed Ge detectors. A time window from −100 to 100 ns was used for prompt $\gamma\gamma$ coincidences in the GS. The typical energy resolution for the GS was ∼3.5 keV (FWHM) for γ-ray energies around 300 keV. The recoil-decay tagging (RDT) [28,29] and the isomer-decay tagging (IDT) techniques [30] were used to provide unambiguous γ-ray assignment to specific nuclide.

New isomeric decay A part of the α-decay spectrum relevant to ^{187}Pb is shown in the inset (a) of Fig. 1. The structure at 6220 to 6264 keV, with ∼ 4.3 × 10^4 decays, corresponds to the partial or full energy summing in the DSSD of the 6194-keV α decay of ^{187g}Pb (relative intensity $I_{\alpha,\mathrm{rel}}$ ∼60% [19]) and ∼ 54-64 keV L/M-shell conversion electrons (CE) resulting from the strong conversion of the known coincident 67-keV $E2$ transition [19]. The 5993-keV decay of ^{187g}Pb ($I_{\alpha,\mathrm{rel}}$ ∼40%) could not be used in the analysis, due to strong contamination from the 5988-keV decay of ^{188}Pb. The peak at 6080(4) keV is associated with the α decay of the $13/2^+$ isomeric state in ^{187}Pb (the evaluated value is 6077(7) keV [20,21]). The population ratio of ^{187m}Pb/^{187g}Pb is ∼ 1.7 : 1, after normalization for the corresponding α-decay branching ratios.

The main panel of Fig. 1 shows the energy spectrum of delayed γ rays registered in X-array, within 20 μs of the implantation of EVRs and followed by the 6220- and 6264-keV (α+CE) summing peaks of ^{187g}Pb (ΔT(EVRs - α)≤ 30 s). A 307.9(1)-keV γ ray was assigned as originating from the decay of a new isomeric state in ^{187}Pb, to the $3/2^-_{gs}$. The half-life of the isomer is determined to be 5.15(15) μs, as shown in inset (b) of Fig. 1. We note that no μs isomers were observed in ^{187}Pb in the previous delayed γ-ray study [31], though the employed detection and electronics system would have allowed the identification of isomeric states with half-lives up to 50 μs.

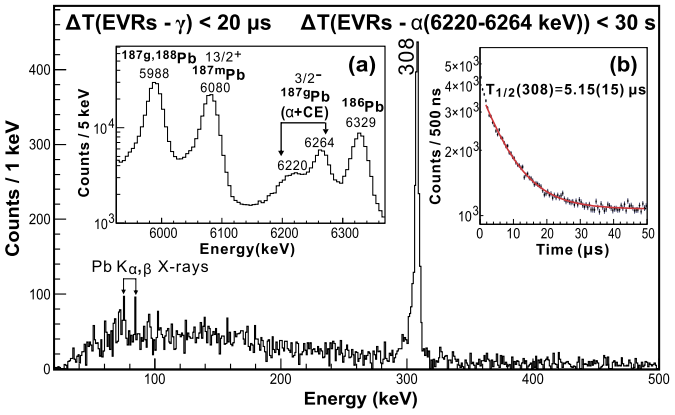

Fig. 1. The main panel: the delayed γ-ray spectrum in the X-array obtained by tagging on the 6220–6264-keV region shown the inset (a). The EVRs-γ and EVRs-α (6220-6264) correlation time intervals are 20 μs and 30 s, respectively. Inset (a): a part of the α-decay spectrum, relevant for ^{187g,m}Pb. The deduced energies are based on the DSSD calibration described in the text. Inset (b): the time distribution and the associated fit by an exponential function with a constant background for the delayed 308-keV transition in ^{187}Pb. In order to have higher statistics, the EVRs-α correlation condition is not used here. The first 2 μs of the time distribution was omitted from the fit to avoid the Compton background from the γ decay of known sub-μs isomeric states in ^{187}Tl and ^{188}Pb [31].

As no γ rays were found in coincidence with the 308-keV transition in the $\gamma\gamma$ coincidence analysis, we assume that all Pb $K_{\alpha,\,\beta}$ X-rays in Fig. 1 originate from the conversion of this delayed transition. Due to low X-ray statistics, only an upper limit of the K-shell conversion coefficient, $\alpha_K(308) < 0.07$, could be deduced, by comparing the number of the full-energy 308-keV decays with the upper limit number of X-rays in Fig. 1 after normalizing for the corresponding γ-ray and X-ray detection efficiencies. The theoretical conversion coefficients [32] for different multipolarities of the 308-keV transition are $\alpha_K(E1) = 0.02$, $\alpha_K(E2) = 0.06$, $\alpha_K(E3) = 0.16$, $\alpha_K(M1) = 0.33$ and $\alpha_K(M2) = 1.12$. Therefore, we rule out $E3$, $M1$ and $M2$ multipolarities, while a pure $E1$ or $E2$ remains possible. Further discussion on the multipolarity of the 308-keV transition will be given in Sec. 3.

Band 1 To search for prompt γ rays in ^{187}Pb, both the IDT and RDT methods were used. Fig. 2(a) and (b) show the background-subtracted prompt GS γ-ray spectra obtained by tagging on the delayed 308-keV γ line (IDT method) and the 6220–6264-keV α group (RDT method), respectively. The IDT analysis provided the cleaner identification of several new γ rays attributed to ^{187}Pb, i.e. 243.8(2)-, 302.2(2)-, 329.3(3)-, 369.3(3)-, 405.7(4)-, 440.7(4)-, 474.4(5)-, 505.3(5)- and 535.4(5)-keV lines. The same γ rays, albeit with lower intensity, are also seen in the RDT spectrum in Fig. 2(b), where a gate on the 6220–6264-keV $(\alpha + CE)$ group was applied with the time difference of ΔT(EVRs - α)$\leq$ 30 s. Taken together, this proves that the de-excitation from higher-lying states proceeds, at least partially, via the new isomer.

Based on the $\gamma\gamma$ coincidence analysis for these transitions, shown in Fig. 3(a), (b) and on the comparison to the $7/2^-[514]$ band in the isotone ^{185}Hg (see Sec. 3), a rotational band built on the isomer was established, see Band 1 in Fig. 4. The two signature branches (shown as Band 1(a) and Band 1(b)) are linked at the bottom via weak 95.0(10)-, 149.4(5)- and 153.0(10)-keV transitions, seen in Fig. 2(a) and Fig. 3(a), (b). No transitions from Band 1 are found in coincidences with the 375-keV γ ray deexciting the $(3/2^-_2)$ state, see e.g. Fig. 3(a), (b), thus states from Band 1 do not decay to this state.

Band 2 Apart from the γ rays in Band 1, several additional γ rays, labeled in bold red text in Fig. 2(b), i.e. 283.3(5)-, 308.1(3)-,

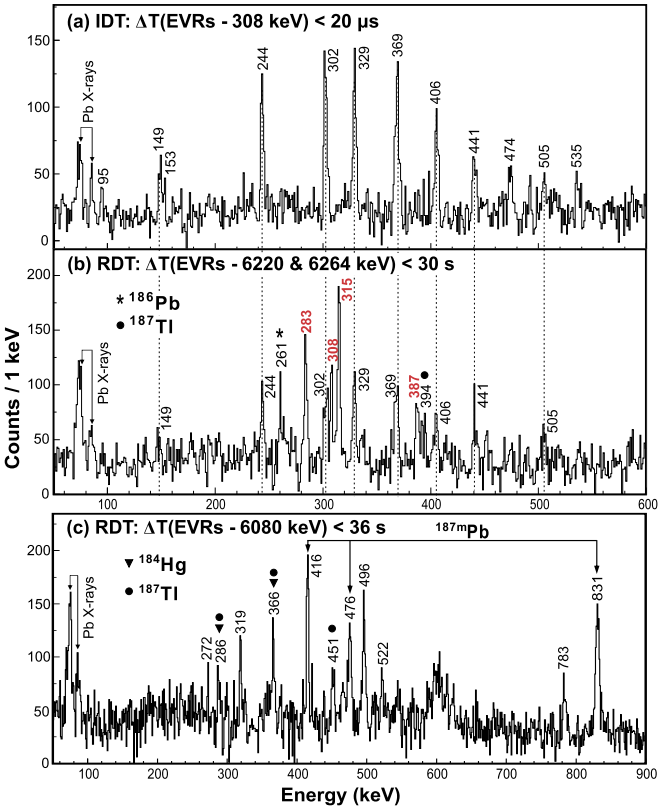

Fig. 2. (a) The background-subtracted prompt γ-ray spectrum in GS obtained by tagging on the delayed 308-keV γ line. (b) The same, but with a tag on the 6220–6264-keV $(\alpha + CE)$ group belonging to ^{187g}Pb. The γ rays labeled in bold red text are not seen in Fig. 2(a), see main text for details. (c) The same, but with a tag on the 6080-keV α decay of ^{187m}Pb. The γ rays from the known band on top of the $13/2^+$ state in ^{187}Pb [12] and the known contaminants are labeled in panel (c). The tagging time intervals for IDT and RDT methods are indicated in the panel titles.

314.7(3)- and 387.4(5)-keV, are also observed, which are not seen in Fig. 2(a). Based on the prompt $\gamma\gamma$ coincidence analysis we proved that they are all in mutual coincidences, thus forming a prompt cascade, labeled as Band 2 in Fig. 4. In addition, Fig. 3(c) shows that the 315-keV line is a doublet. Similar to Band 1, no 375-keV γ ray is seen in coincidence with this cascade, see e.g. Fig. 3(c). Based on the above arguments, we assigned this cascade of five γ rays as feeding directly to the $3/2^-_{gs}$ and bypassing the new isomer. The relative ordering of the γ rays within the cascade could not be established due to their similar intensities after normalization on the γ-ray efficiency and assuming comparable conversion coefficients.

We note that the 308-keV γ line is present in both the delayed spectrum in Fig. 1 and the prompt RDT spectrum in Fig. 2(b). Based on the different time behaviors of the 307.9(1)- and 308.1(3)-keV decays, and on a small energy difference between them (albeit still within the uncertainties), we propose that they are two different transitions, the former is delayed, de-exciting the 5.15(15) μs isomer, and the latter is prompt in Band 2.

The known band above ^{187m}Pb Fig. 2(c) shows the background-subtracted RDT spectrum tagged with the 6080-keV decay of ^{187m}Pb. The 830.6(3)-, 415.8(2)- and 475.5(3)-keV γ rays match well to three known transitions on top of the $13/2^+$ isomer [12]. No new transitions were found for this band based on our $\gamma\gamma$ coincidence analysis.

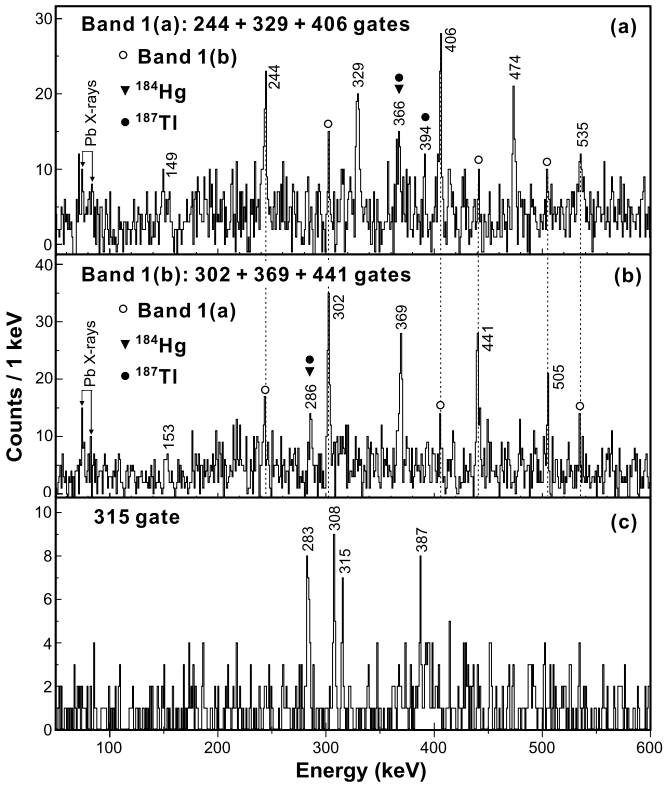

Fig. 3. (a) γ-ray energy spectrum for Band 1(a) from the sum of γ-gates shown, for the IDT + RDT analysis. (b) A similar spectrum for transitions within Band 1(b). (c) The 315-keV gated spectrum based on the RDT analysis, proving the doublet nature of the 315-keV transition and the absence of coincidences with the 375-keV decay from the $(3/2^-_2)$ state. Peaks are labeled with their energies in keV. The gate energies are indicated in the panel titles and the contaminants are marked by full symbols.

The known $(3/2^-_2)$ *state* No evidence for the 375-keV γ ray corresponding to the de-excitation from the $(3/2^-_2)$ state, proposed in [17] as a bandhead of an oblate configuration, was found in our work. This fact indicates that the population of the $(3/2^-_2)$ state is much weaker than that of Bands 1 and 2.

3. Discussion

Fig. 4 shows the strongly-coupled prolate $7/2^-[514]$ band in the isotone ^{185}Hg [33]. The similarity between the new Band 1 in ^{187}Pb and the band in ^{185}Hg (also, in ^{183}Hg, see below) is striking, with nearly identical transition energies in both bands. On these grounds, we assign the same $7/2^-[514]$ Nilsson configuration to the bandhead of Band 1 in ^{187}Pb and respective spin-parity values for the excited states within the band. This assignment leads to an $E2$ multipolarity for the delayed 308-keV $(7/2^-)\rightarrow 3/2^-_{gs}$ decay, which is consistent with the upper limit of the conversion coefficient deduced in Sec. 2, which suggested a pure $E1$ or $E2$. The 5.15(15)-μs half-life establishes a strongly-hindered character for the 308-keV transition, with $B(E2, 308\ \text{keV}) = 5.6(2) \times 10^{-4}$ W.u. The hindrance could result from a presumed significant shape difference between the prolate-deformed $7/2^-[514]$ Nilsson state and the nearly spherical $3/2^-_{gs}$. Thus the 308-keV state can be considered as a shape isomer in ^{187}Pb. Band 2 possibly represents an excited structure based on the spherical $3/2^-_{gs}$.

Apart from ^{185}Hg, we also note a close similarity of Band 1 in ^{187}Pb to the known $7/2^-[514]$ band in ^{183}Hg [34]. The nearly identical properties of the $7/2^-$ bands in ^{183,185}Hg were discussed in Ref. [35]. To compare the rotational properties of the $(7/2^-)$ bands in ^{187}Pb and ^{183,185}Hg, the experimental aligned angular

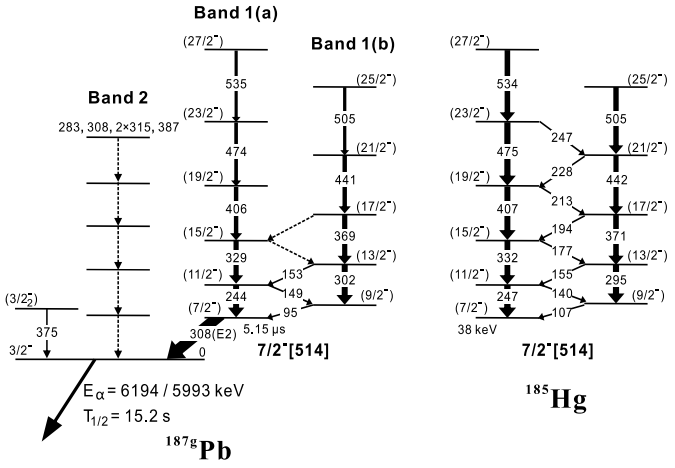

Fig. 4. Proposed level scheme for ^{187g}Pb and partial level scheme of ^{185}Hg [33]. Tentative placements in ^{187}Pb are indicated by dashed lines and tentative spin-parity assignments are given in parentheses. The prompt cascade of five γ rays (including the doublet at 315 keV) is schematically shown for the Band 2 and the order of transitions is not known, see main text for details. The $(3/2^-_2)$ state at 375 keV was identified in [17] and is shown here for completeness.

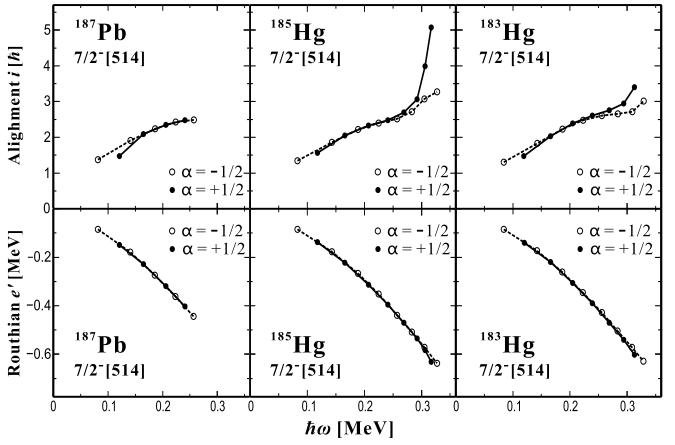

Fig. 5. The aligned angular momenta i (top row) and experimental Routhians (bottom row) of Band 1 in ^{187}Pb in comparison with the $7/2^-[514]$ bands in ^{183,185}Hg. The open circles and solid circles represent the favored and unfavored signatures of the bands, respectively. The reference parameters of the Harris formula [36] for the moment of inertia are $J_0 = 25.1\ \hbar^2/(\text{MeV})$ and $J_1 = 209\ \hbar^4/(\text{MeV})^3$ [37], and they are used for all bands.

momenta i and Routhians e' are plotted as a function of the rotational frequency, $\hbar\omega$, in Fig. 5. No signature splitting is observed for these bands. The angular momentum alignment is very similar and gradual at low rotational frequencies for these 3 cases, but suddenly increases as the rotational frequency approaches 0.3 MeV in ^{183,185}Hg. Unfortunately, the higher-spin members of the $(7/2^-)$ band in ^{187}Pb have not yet been observed due to the low statistics. The experimental Routhians of these bands are also consistent with each other, further confirming that the three bands are almost identical and consequently based on the same configuration. The similarity between the $(7/2^-)$ prolate structures in ^{187}Pb and ^{183,185}Hg implies that the addition of two extra protons to the prolate Hg core does not affect the rotational properties of the band built on the $\nu 7/2^-[514]$ configuration.

The $B(M1)/B(E2)$ branching ratios were extracted for Band 1 in ^{187}Pb by using the same assumptions/relations as for the ^{185}Hg analysis in Ref. [33]. The deduced experimental upper limit values of the ratios are 0.06(2) for the initial spin $I_i = 11/2$, and 0.04(2) for $I_i = 13/2$. The calculated values of the $B(M1)/B(E2)$ ratios are 0.07 with $I_i = 11/2$ and 0.05 with $I_i = 13/2$, respectively. These

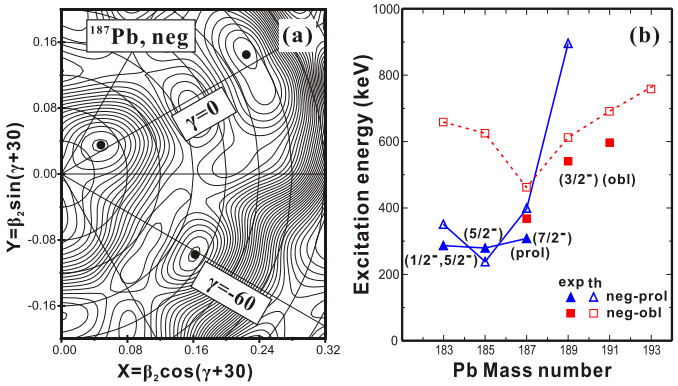

Fig. 6. (a) The PES for ^{187}Pb, negative-parity configurations. The near spherical gs ($\beta_2 \approx 0.06$, $\gamma = 0$), and excited oblate and prolate minima are indicated by black circles. Here, $\gamma = 0$ corresponds to prolate shape and $\gamma = -60$ to oblate shape. The energy distance between contour lines is 100 keV. (b) systematics of excitation energies of the deformed minima in the odd-A $^{183-193}$Pb isotopes with respect to the calculated gs. The experimental and calculated excitation energies (the latter taken from PES calculations) are shown by solid and open symbols, respectively. The values for the prolate and oblate minima are indicated by triangles and squares, respectively. The experimental data are taken from [5,15–18] and the present work.

are in agreement with each other for the $7/2^-$ [514] band in ^{187}Pb, and consequently supporting its $7/2^-$[514] assignment and prolate deformation. The deduction of $B(M1)/B(E2)$ ratios is given in Supplemental Material.

To better understand the low-lying states in ^{187}Pb, we have performed PES calculations for $^{183-193}$Pb ($N = 101$–111) nuclei. Calculations used the deformed Woods-Saxon potential and followed the prescription in Ref. [17]. We refer the reader to Fig. 7 of Ref. [17], where, based on the PES calculations, triple shape coexistence for positive-parity states in ^{187}Pb was discussed. Here we focus on the negative-parity states with the new experimental information obtained in the present work. Fig. 6 (a) shows the calculated PES for negative-parity states in ^{187}Pb, where the 3 coexisting minima - spherical, oblate and prolate can clearly be seen.

The two presently known lowest negative-parity states above the spherical $3/2^-_{gs}$ of ^{187}Pb are the prolate 308-keV ($7/2^-$) state identified in this work, and presumably the oblate 375-keV ($3/2^-_2$) state [23,17], see Fig. 4. Taken together, a pattern of triple shape coexistence is now also evident for the negative-parity states in this nucleus. However, we remind the reader that the shape and configuration assignment to the excited states in [17] should be taken with caution, as it was based on hindrance factor values for α decay, complemented with PES and particle-rotor calculations.

Fig. 6 (b) compares the calculated and experimental excitation energies, for the lowest negative-parity states (bandheads) in odd-A $^{183-191}$Pb isotopes. The calculated excitation energies were extracted from the PES calculations relative to the respective gs, e.g. from Fig. 6 (a) for ^{187}Pb. Good agreement between predicted and measured excitation energies for the oblate ($3/2^-$) states in ^{187,189,191}Pb is visible (open and closed squares in Fig. 6 (b)), with a deviation not exceeding 100 keV, and a predicted minimum occurs around the mid-shell at $N = 104$.

A striking steep drop in the excitation energy of the prolate bandheads (open triangles in Fig. 6 (b)) is also predicted, with a minimum around ^{185}Pb. In ^{183,185,187}Pb, where such states are experimentally known, the predicted energies match quite well (within ≈100 keV) to the experimental energies, albeit the experimental trend is flatter. We would like to point out that these states in ^{183,185}Pb were observed via α-decay studies of the parent Po isotopes at the velocity filter SHIP. These are tentatively interpreted as prolate states based on the observed α-decay pattern and on the PES and particle-rotor calculations, see details in [15,16], and thus the nature of these states in ^{183,185}Pb still requires a further confirmation. It would also be important to search for such a prolate configuration in ^{189}Pb in order to confirm the predicted steep trend.

The proximity of the experimental and calculated energies for the negative-parity prolate bandhead further supports our assignment of the 308-keV state as the bandhead of the prolate configuration. Therefore, the low-lying triple shape coexistence pattern in ^{187}Pb is similar to that in the neighboring ^{186}Pb, in which the two deformed low-lying 0^+ states were found above the spherical 0^+ gs [4].

However, an important difference can be noted between the odd-A and even-even Pb isotopes. The experimental excitation energies of the deformed 0^+ states in ^{186,188}Pb are around 530 – 720 keV, about a factor of two larger than that of the known prolate bandheads in ^{183,185,187}Pb. This effect can be related to the difference in the neutron pairing gaps, Δ, for spherical and deformed configurations. Below, we outline this link by a schematic procedure for the prolate band in ^{187}Pb.

Following the procedure of Ref. [38], the bandhead energy E_i in an odd-A Pb nucleus can be written as: $E_i = E_{i,0} + \Delta_i$, where the index i stands for "s" (spherical), "o" (oblate) or "p" (prolate), the $E_{i,0}$ is a fictitious energy when blocking is switched off. From a mean-field point of view, $E_{i,0}$ corresponds to the energy of the fully paired many-particle wave function, whereas Δ_i is the energy gain due to the blocking of an orbital by the odd neutron. It is important to note that Δ_i depends on the deformation of the underlying configuration. Due to a relatively weak dependence of the $0^+_{2,3}$ energies on the neutron number in ^{186,188}Pb, we use the energies of these states in ^{186}Pb as a reasonable approximation for $E_{i,0}$. Let us first consider the spherical gs of ^{187}Pb. Assuming for simplicity $E_{s,0} = 0$, we obtain $E_s = \Delta_s = 1259$ keV; the spherical pairing gap Δ_s was calculated by the standard three-point formula using the binding energies for the ground states of ^{186,187,188}Pb [39]. Deformed oblate and prolate 0^+ states in the core ^{186}Pb are at 532 and 650 keV [4], respectively, with strong mixing between them [40]. Therefore, one might expect that the fictitious (without blocking) prolate bandhead in ^{187}Pb is situated somewhere between the observed mixed 0^+ states: $E_{p,0} = 595(60)$ keV. The neutron pairing gap for the deformed $7/2^-$[514] state can be determined from the binding energies of the isotonic platinum nuclei, $\Delta_p(7/2^-[514]) = 1011$ keV. Thus, we obtain $E_p = 595(60) + 1011 = 1606(60)$ keV. Correspondingly, the expected excitation energy of the $7/2^-$[514] state is $E(7/2^-[514], ^{187}\text{Pb}) = E_p - E_s = 347(60)$ keV, which in good qualitative agreement with the experimental data. Therefore, we conclude that, despite rather crude approximations employed in this procedure, it provides a reasonable interpretation of the lower energies of the deformed bandheads in the odd-A nuclei.

4. Summary

In summary, we have identified a new ($7/2^-$) isomeric state at 308 keV above the spherical $3/2^-_{gs}$ of ^{187}Pb, with a half-life of 5.15(15) µs. By using the IDT and RDT methods, a strongly-coupled rotational band built on the isomer was observed, which is nearly identical to the strongly-coupled prolate $7/2^-$[514] bands in ^{183,185}Hg, in both transition energies and rotational behavior. In addition, we performed PES calculations, which predict a triple spherical-oblate-prolate shape coexistence in ^{187}Pb, similar to that in the even-even neighbor ^{186}Pb [4]. Taken together with an earlier identification of a presumably oblate ($3/2^-_2$) excited state at 375 keV, triple shape coexistence is now established for the negative-parity states in ^{187}Pb, as it was earlier proposed for the positive-parity states [17]. The hindered nature of the 308-keV $E2$ decay reflects the strong shape and deformation difference between the

$(7/2^-)$ prolate isomeric state and spherical $3/2^-_{gs}$ in ^{187}Pb, implying that the former state is a shape isomer.

Declaration of competing interest

The authors declare that they have no known competing financial interests or personal relationships that could have appeared to influence the work reported in this paper.

Acknowledgements

This work was supported by the Strategic Priority Research Program of Chinese Academy of Sciences (Grant No. XDB34000000), the National Key R&D Program of China (Contract No. 2018YFA0404402), the National Natural Science Foundation of China (Grants No. 12135004, No. 11635003, No. 11961141004, No. 11735017 and No. U2032138). UK personnel are grateful for financial support from the STFC and A.N. Andreyev is funded by the Chinese Academy of Sciences President's International Fellowship Initiative (Grant No. 2020VMA0017). This work was also supported by the U.S. Department of Energy, Office of Nuclear Physics, under Contract No. DE-AC02-06CH11357 and Grants No. DE-FG02-94ER41041 (UNC) and DE-FG02-97ER41033 (TUNL). This research used resources of ANL's ATLAS facility, which is a DOE Office of Science User Facility. We thank the Target Labor team of GSI for preparing the targets for the experiment.

Appendix A. Supplementary material

Supplementary material related to this article can be found online at https://doi.org/10.1016/j.physletb.2022.137129.

References

[1] K. Heyde, J.L. Wood, Rev. Mod. Phys. 83 (2011) 1467–1521, https://doi.org/10.1103/RevModPhys.83.1467.
[2] J.L. Wood, K. Heyde, J. Phys. G, Nucl. Part. Phys. 43 (2) (2016) 020402, https://doi.org/10.1088/0954-3899/43/2/020402.
[3] R. Julin, T. Grahn, J. Pakarinen, P. Rahkila, J. Phys. G, Nucl. Part. Phys. 43 (2) (2016) 024004, https://doi.org/10.1088/0954-3899/43/2/024004.
[4] A.N. Andreyev, D. Ackermann, J. Gerl, F.P. Heßberger, S. Hofmann, A. Kleinbo, S. Reshitko, C. Schlegel, H. Schaffner, P. Cagarda, G. Mu, Nature 405 (May 2000) 186–189, https://doi.org/10.1038/35013012.
[5] K. Van de Vel, A.N. Andreyev, D. Ackermann, H.J. Boardman, P. Cagarda, J. Gerl, F.P. Heßberger, S. Hofmann, M. Huyse, D. Karlgren, I. Kojouharov, M. Leino, B. Lommel, G. Münzenberg, C. Moore, R.D. Page, S. Saro, P. Van Duppen, R. Wyss, Phys. Rev. C 68 (2003) 054311, https://doi.org/10.1103/PhysRevC.68.054311.
[6] G.D. Dracoulis, A.P. Byrne, A.M. Baxter, P.M. Davidson, T. Kibédi, T.R. McGoram, R.A. Bark, S.M. Mullins, Phys. Rev. C 60 (1999) 014303, https://doi.org/10.1103/PhysRevC.60.014303.
[7] K. Heyde, C. De Coster, J. Ryckebusch, M. Waroquier, Phys. Lett. B 218 (3) (1989) 287–290, https://doi.org/10.1016/0370-2693(89)91582-7.
[8] R. Bengtsson, W. Nazarewicz, Z. Phys. A, At. Nucl. 334 (3) (1989) 269–276, https://doi.org/10.1007/BF01284554.
[9] H. De Witte, A.N. Andreyev, N. Barré, M. Bender, T.E. Cocolios, S. Dean, D. Fedorov, V.N. Fedoseyev, L.M. Fraile, S. Franchoo, V. Hellemans, P.H. Heenen, K. Heyde, G. Huber, M. Huyse, H. Jeppessen, U. Köster, P. Kunz, S.R. Lesher, B.A. Marsh, I. Mukha, B. Roussière, J. Sauvage, M. Seliverstov, I. Stefanescu, E. Tengborn, K. Van de Vel, J. Van de Walle, P. Van Duppen, Y. Volkov, Phys. Rev. Lett. 98 (2007) 112502, https://doi.org/10.1103/PhysRevLett.98.112502.
[10] R.R. Rodríguez-Guzmán, J.L. Egido, L.M. Robledo, Phys. Rev. C 69 (2004) 054319, https://doi.org/10.1103/PhysRevC.69.054319.
[11] A.M. Baxter, A.P. Byrne, G.D. Dracoulis, P.M. Davidson, T. Kibédi, R.V.F. Janssens, M.P. Carpenter, C.N. Davids, T.L. Khoo, T. Lauritsen, Phys. Rev. C 71 (2005) 054302, https://doi.org/10.1103/PhysRevC.71.054302.
[12] A.M. Baxter, A.P. Byrne, G.D. Dracoulis, P.M. Davidson, T.R. McGoram, P.H. Regan, C. Chandler, W. Gelletly, C. Wheldon, R. Julin, J.F.C. Cocks, K. Helariutta, P. Jones, S. Juutinen, H. Kankaanpää, H. Kettunen, P. Kuusiniemi, M. Leino, M. Muikku, A. Savelius, R.V.F. Janssens, T. Brown, M.P. Carpenter, C.N. Davids, T. Lauritsen, D. Nisius, P.T. Greenlees, Phys. Rev. C 58 (1998) 2671–2676, https://doi.org/10.1103/PhysRevC.58.2671.
[13] S. Chmel, F. Brandolini, R.V. Ribas, G. Baldsiefen, A. Görgen, M. De Poli, P. Pavan, H. Hübel, Phys. Rev. Lett. 79 (1997) 2002–2005, https://doi.org/10.1103/PhysRevLett.79.2002.
[14] J. Pakarinen, A.N. Andreyev, R. Julin, S. Juutinen, S. Antalic, L. Bianco, I.G. Darby, S. Eeckhaudt, T. Grahn, P.T. Greenlees, D.G. Jenkins, P. Jones, P. Joshi, H. Kettunen, M. Leino, A.P. Leppänen, P. Nieminen, M. Nyman, R.D. Page, J. Perkowski, P.M. Raddon, P. Rahkila, D. Rostron, J. Saren, C. Scholey, J. Sorri, B. Streicher, J. Uusitalo, K.V. de Vel, M. Venhart, R. Wadsworth, D.R. Wiseman, Phys. Rev. C 80 (2009) 031303, https://doi.org/10.1103/PhysRevC.80.031303.
[15] A.N. Andreyev, S. Antalic, D. Ackermann, S. Franchoo, F.P. Heßberger, S. Hofmann, M. Huyse, I. Kojouharov, B. Kindler, P. Kuusiniemi, S.R. Lesher, B. Lommel, R. Mann, G. Münzenberg, K. Nishio, R.D. Page, J.J. Ressler, B. Streicher, S. Saro, B. Sulignano, P.V. Duppen, D. Wiseman, R. Wyss, Phys. Rev. C 73 (2006) 044324, https://doi.org/10.1103/PhysRevC.73.044324.
[16] K. Van de Vel, A.N. Andreyev, D. Ackermann, H.J. Boardman, P. Cagarda, J. Gerl, F.P. Heßberger, S. Hofmann, M. Huyse, D. Karlgren, I. Kojouharov, M. Leino, B. Lommel, G. Münzenberg, C. Moore, R.D. Page, S. Saro, P. Van Duppen, R. Wyss, Eur. Phys. J. A 24 (1) (2005) 57–62, https://doi.org/10.1140/epja/i2004-10124-7.
[17] A.N. Andreyev, M. Huyse, K. Van de Vel, P. Van Duppen, O. Dorvaux, P. Greenlees, K. Helariutta, P. Jones, R. Julin, S. Juutinen, H. Kettunen, P. Kuusiniemi, M. Leino, M. Muikku, P. Nieminen, P. Rahkila, J. Uusitalo, R. Wyss, K. Hauschild, Y. Le Coz, Phys. Rev. C 66 (2002) 014313, https://doi.org/10.1103/PhysRevC.66.014313.
[18] K. Van de Vel, A.N. Andreyev, M. Huyse, P. Van Duppen, J.F.C. Cocks, O. Dorvaux, P.T. Greenlees, K. Helariutta, P. Jones, R. Julin, S. Juutinen, H. Kettunen, P. Kuusiniemi, M. Leino, M. Muikku, P. Nieminen, K. Eskola, R. Wyss, Phys. Rev. C 65 (2002) 064301, https://doi.org/10.1103/PhysRevC.65.064301.
[19] P. Misaelides, P. Tidemand-Petersson, U.J. Schrewe, I.S. Grant, R. Kirchner, O. Klepper, I.C. Malcolm, P.J. Nolan, E. Roeckl, W.-D. Schmidt-Ott, J.L. Wood, Z. Phys. A 301 (3) (1981) 199–208, https://doi.org/10.1007/BF01416294.
[20] F.G. Kondev, M. Wang, W.J. Huang, S. Naimi, G. Audi, Chin. Phys. C 45 (2021) 030001, https://doi.org/10.1088/1674-1137/abddae.
[21] W.J. Huang, M. Wang, F.G. Kondev, G. Audi, S. Naimi, Chin. Phys. C 45 (CPC-2021–0034) (2021) 030002, https://doi.org/10.1088/1674-1137/abddb0.
[22] M.D. Seliverstov, A.N. Andreyev, N. Barré, A.E. Barzakh, S. Dean, H. De Witte, D.V. Fedorov, V.N. Fedoseyev, L.M. Fraile, S. Franchoo, J. Genevey, G. Huber, M. Huyse, U. Köster, P. Kunz, S.R. Lesher, B.A. Marsh, I. Mukha, B. Roussière, J. Sauvage, I. Stefanescu, K. Van de Vel, P. Van Duppen, Y.M. Volkov, Eur. Phys. J. A 41 (2009) 315–321, https://doi.org/10.1140/epja/i2009-10817-3.
[23] A.N. Andreyev, M. Huyse, P. Van Duppen, J.F.C. Cocks, K. Helariutta, H. Kettunen, P. Kuusiniemi, M. Leino, W.H. Trzaska, K. Eskola, R. Wyss, Phys. Rev. Lett. 82 (1999) 1819–1822, https://doi.org/10.1103/PhysRevLett.82.1819.
[24] B.B. Back, EPJ Web Conf. 163 (2017) 00003, https://doi.org/10.1051/epjconf/201716300003.
[25] H. Huang, et al., submitted to Phys. Lett. B (2022).
[26] A.J. Mitchell, P.F. Bertone, B. DiGiovine, C.J. Lister, M.P. Carpenter, P. Chowdhury, J.A. Clark, N. D'Olympia, A.Y. Deo, F.G. Kondev, E.A. McCutchan, J. Rohrer, G. Savard, D. Seweryniak, S. Zhu, Nucl. Instrum. Methods Phys. Res., Sect. A, Accel. Spectrom. Detect. Assoc. Equip. 763 (2014) 232–239, https://doi.org/10.1016/j.nima.2014.06.024.
[27] I.-Y. Lee, in: Nuclear Structure in the Nineties, Nucl. Phys. A 520 (1990) c641–c655, https://doi.org/10.1016/0375-9474(90)91181-P.
[28] E.S. Paul, P.J. Woods, T. Davinson, R.D. Page, P.J. Sellin, C.W. Beausang, R.M. Clark, R.A. Cunningham, S.A. Forbes, D.B. Fossan, A. Gizon, J. Gizon, K. Hauschild, I.M. Hibbert, A.N. James, D.R. LaFosse, I. Lazarus, H. Schnare, J. Simpson, R. Wadsworth, M.P. Waring, Phys. Rev. C 51 (1995) 78–87, https://doi.org/10.1103/PhysRevC.51.78.
[29] R.S. Simon, K.-H. Schmidt, F.P. Heßberger, S. Hlavac, M. Honusek, G. Münzenberg, H.-G. Clerc, U. Gollerthan, W. Schwab, Z. Phys. A, At. Nucl. 325 (2) (1986) 197–202, https://doi.org/10.1007/BF01289651.
[30] D.M. Cullen, N. Amzal, A.J. Boston, P.A. Butler, A. Keenan, E.S. Paul, H.C. Scraggs, A.M. Bruce, C.M. Parry, J.F.C. Cocks, K. Helariutta, P.M. Jones, R. Julin, S. Juutinen, H. Kankaanpää, H. Kettunen, P. Kuusiniemi, M. Leino, M. Muikku, A. Savelius, Phys. Rev. C 58 (1998) 846–850, https://doi.org/10.1103/PhysRevC.58.846.
[31] A.P. Byrne, A.M. Baxter, G.D. Dracoulis, S.M. Mullins, T. Kibédi, T.R. McGoram, K. Helariutta, J.F.C. Cocks, P. Jones, R. Julin, S. Juutinen, H. Kankaanpää, H. Kettunen, P. Kuusiniemi, M. Leino, M. Muikku, P. Nieminen, P. Rahkila, A. Savelius, Eur. Phys. J. A 7 (1) (2000) 41–44, https://doi.org/10.1007/s100500050008.
[32] T. Kibédi, T.W. Burrows, M.B. Trzhaskovskaya, P.M. Davidson, C.W. Nestor, Nucl. Instrum. Methods Phys. Res., Sect. A, Accel. Spectrom. Detect. Assoc. Equip. 589 (2) (2008) 202–229, https://doi.org/10.1016/j.nima.2008.02.051.
[33] F. Hannachi, G. Bastin, M.G. Porquet, J.P. Thibaud, C. Bourgeois, L. Hildingsson, N. Perrin, H. Sergolle, F.A. Beck, J.C. Merdinger, Z. Phys. A, At. Nucl. 330 (1) (1988) 15–22, https://doi.org/10.1007/BF01287258.
[34] D.T. Shi, W.C. Ma, A.V. Ramayya, J.H. Hamilton, B.R.S. Babu, J. Kormicki, L. Chaturvedi, Q.H. Lu, L.T. Brown, S.L. Tabor, M.A. Riley, J. Döring, D.E. Archer, T. Brown, S.K. Jewell, R.A. Kaye, O.J. Tekyi-Mensah, P.B. Semmes, Phys. Rev. C 51 (1995) 1720–1725, https://doi.org/10.1103/PhysRevC.51.1720.
[35] K. Bindra, A. Ramayya, W. Ma, B. Babu, J. Hamilton, L. Chaturvedi, J. Kormicki, R. Janssens, C. Davids, I. Ahmad, I. Bearden, M. Carpenter, W. Chung, D. Henderson, R. Henry, T. Khoo, T. Lauritsen, Y. Liang, H. Penttila, F. Soramel, C. Baktash, W. Nazarewicz, J. Sheikh, Phys. Lett. B 318 (1) (1993) 41–46, https://doi.org/10.1016/0370-2693(93)91781-H.

[36] S.M. Harris, Phys. Rev. 138 (1965) B509–B513, https://doi.org/10.1103/PhysRev.138.B509.
[37] A.M. Baxter, A.P. Byrne, G.D. Dracoulis, R.V.F. Janssens, I.G. Bearden, R.G. Henry, D. Nisius, C.N. Davids, T.L. Khoo, T. Lauritsen, H. Penttilä, D.J. Henderson, M.P. Carpenter, Phys. Rev. C 48 (1993) R2140–R2143, https://doi.org/10.1103/PhysRevC.48.R2140.
[38] D.G. Madland, J. Nix, Nucl. Phys. A 476 (1) (1988) 1–38, https://doi.org/10.1016/0375-9474(88)90370-3.
[39] M. Wang, W.J. Huang, F.G. Kondev, G. Audi, S. Naimi, Chin. Phys. C 45 (3) (2021) 030002, https://doi.org/10.1088/1674-1137/abddaf.
[40] M. Bender, K. Rutz, P.G. Reinhard, J.A. Maruhn, Eur. Phys. J. A 8 (1) (2000) 59–75, https://doi.org/10.1007/s10050-000-4504-z.